

## A Nanofluidic Switching Device

Roger Karlsson,<sup>#</sup> Anders Karlsson,<sup>#</sup> and Owe Orwar<sup>\*,§</sup>

Department of Physical Chemistry and Microtechnology Center, Chalmers University of Technology, SE-412 96 Göteborg, Sweden, and Department of Chemistry, Göteborg University, SE-412 96 Göteborg, Sweden

Received February 26, 2003; E-mail: orwar@phc.chalmers.se

Controlled aqueous flow in channels with characteristic length scales in the low nanometer range,  $\sim 10$ – $100$  nm (nanofluidics), has a potential to provide new powerful tools that can give unique insight into and understanding of how chemical reactions occur and how fluids behave in confined geometries.<sup>1,2</sup> Appropriately designed nanofluidic systems could serve as important platforms for studies of single-molecule dynamics,<sup>3</sup> enzyme-catalyzed reactions,<sup>4</sup> single-file diffusion,<sup>5</sup> and single-molecule sequencing and synthesis. Furthermore, such systems can provide an understanding of materials transport and reactions in biological systems that occur on these length scales and, as of today, are poorly understood.<sup>6,7</sup>

We have constructed networks in lipid bilayer membranes consisting of surface-immobilized containers ( $5$ – $10$   $\mu\text{m}$  radius) conjugated with suspended nanotubes ( $\sim 100$  nm in diameter and  $20$ – $30$   $\mu\text{m}$  in length). A system of spherical containers connected by thin tubes is energetically favored due to minimization of the elastic energy in the lipid bilayer membrane, where in-plane tension or stretching competes with bending of the membrane. The networks have controlled geometry and topology,<sup>8–10</sup> and fluid flow can be controlled by controlling the surface free energy, e.g., the membrane tension ( $\sigma$ ) of the device material itself.<sup>11</sup> The membrane tension can, for example, be locally increased by using carbon microfibers working as tweezers, controlled by micromanipulators.<sup>8</sup>

Here, we present a nanofluidic switching function based on creating a membrane tension gradient using a two-point perturbation technique, which allows directed transport between any two or several containers in a network. This capability is essential for controlled routing and switching of fluid directions in networks with more than two containers and will thus open up possibilities for large-scale integration in nanofluidic systems.

If surface tension is increased at a single container, in a system of  $n$  containers we would have one drain (at the point of increased tension) and  $n - 1$  sources for the lipid membrane in a symmetrical case. For example, if surface tension is increased,  $+\sigma$ , in vesicle no. 4 in Figure 1 a, membrane and fluid will symmetrically be moved from vesicles 1–3. To be able to route material with directionality in such multicontainer networks, we developed a two-point perturbation technique. With this method, the membrane tension of one surface-adhered vesicle was decreased by adding excess membrane material through insertion of membrane from a nanotube-connected donor vesicle<sup>12</sup> (denoted by  $\delta$  in Figure 1a and d), simultaneously as the membrane tension in another vesicle was increased by mechanical excitation using a carbon microfiber as tweezers. We thereby created a difference in tension between two containers that was much larger than for all the other connected containers (Figure 1b). For the addition of membrane material, we

used  $5$ - $\mu\text{m}$ -diameter donor vesicles,  $\delta$ , which were allowed to merge (by size expansion or micromanipulator-controlled transport of  $\delta$ ) with the surface-adhered vesicles having a typical size of  $15$   $\mu\text{m}$  in diameter. This will lead to an 8% surplus membrane area of the resulting product vesicle. The excess membrane drops the membrane tension below the limit where membrane bending dominates ( $< 0.5$  mN/m),<sup>13</sup> subsequently leading to undulations on the vesicle and nanotube membrane (Figure 1b), which are transformed into 2-fold open-ended nanotube-integrated vesicles, having a typical radius of  $0.5$   $\mu\text{m}$  (Figure 1c).

Importantly, the newly formed vesicles will have the same contents as the surface-immobilized vesicle from which they were formed. The content of the surface-immobilized vesicle can change when remerging with the donor vesicle,  $\delta$ , and if so, the diffusive and convective mixing time scale for the internal fluids of the two vesicles has to be taken into account. If the mixing times are much longer than the time required for the system to return to the original shape, then the nanotube-integrated vesicles will have the same contents as the surface-adhered vesicle *before* the donor vesicle was allowed to remerge with it. The particular dynamics and mechanics of the formation of the nanotube-integrated vesicles are described elsewhere,<sup>14</sup> and are not important in the forthcoming discussion.

A three-container network was constructed to demonstrate the switching feature and liquid routing capability in these devices (Figure 1d–j). Vesicles (white arrows) were created on two nanotubes, conjugated to the three containers, shown schematically in Figure 1d–f and in the corresponding Nomarski differential interference contrast (DIC) microscopy images in Figure 1g–j. Magnifications of the nanotube sections were made, showing the integrated vesicles more clearly (see insets). By locally controlling the membrane tension, a flow of membrane material could be created across the nanotubes (black arrows). In general, the transport rate of lipid scales as the ratio between the difference in membrane tension over the nanotube and the effective viscosity of the system.<sup>11,15</sup> The lipid velocity was in the range of  $30$   $\mu\text{m}/\text{s}$ , and transfer of material could be achieved in the time scale of a few seconds. The nanotube-integrated vesicles moved with the lipid flow, and the system could therefore perform vesicle injections into selected target containers. To illustrate the injection, fluorescent dextrane was loaded into nanotube-integrated vesicles and moved to another surface-adhered vesicle (Figure 1k), where it released its contents (Figure 1l). The majority of the liquid is transported in the form of the small vesicular structures ( $10^{-15}$ – $10^{-18}$  L) along the nanotubes, though a fraction is transported inside the nanotubes.<sup>11</sup> Since the sizes of the vesicles can be measured, the transferred amount of material can be determined.

Our system can be made to have few or many containers with a more or less intricate connectivity.<sup>8,9,11,12</sup> Using the two-point

<sup>§</sup> Chalmers University of Technology.

<sup>#</sup> Göteborg University.

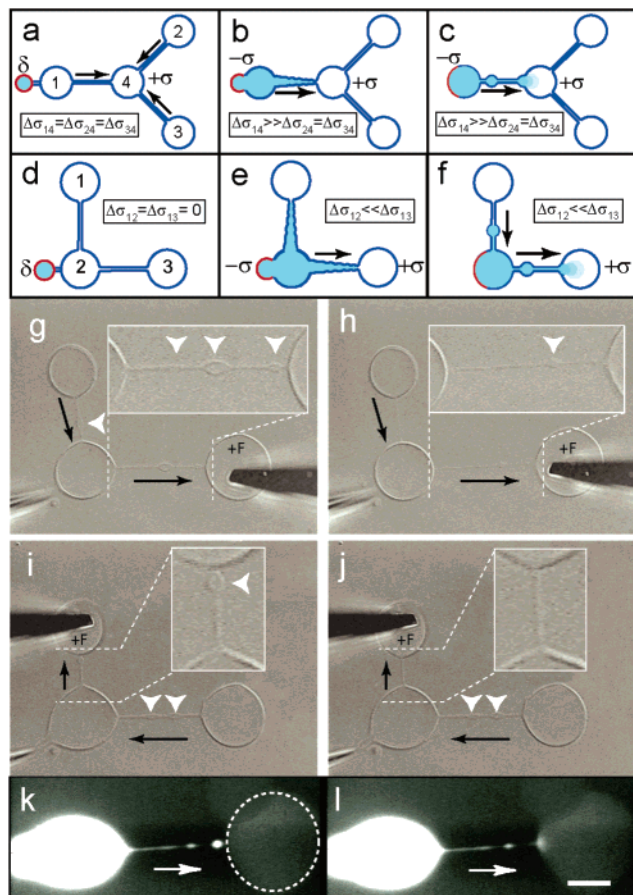


**Figure 1.** (a) Schematic showing a four-container nanotube network (top view). If the tension,  $\sigma$ , in the containers is the same, there is no active transport of lipid membrane material across the nanotubes. If the tension is increased in vesicle 4 ( $+\sigma$ ), lipids will start to flow from all other vesicles (one drain and three sources). (b) By lowering the tension in one other vesicle ( $-\sigma$ ) through introduction of surplus membrane, the difference in tension will be largest between these vesicles. Addition of membrane material to a surface-immobilized vesicle can be performed by allowing a nanotube-connected vesicle (red membrane and blue interior), here denoted by  $\delta$ , to remerge with it. This will result in a shape transformation and dilation of the nanotube connecting the two surface-immobilized vesicles. (c) Due to energy minimization, the system adopts a conformation of surface-adhered vesicles connected by thin tubes, and the excess fluid which has entered the deformed nanotube will be trapped and vesicles (500 nm to 5  $\mu\text{m}$  in diameter) will be formed. The membrane tension of a target vesicle is increased by shape deformation using a micromanipulator-controlled carbon fiber, and a concomitant lipid flow toward it is created. The nanotube-integrated vesicles follow the lipid flow and inject their contents into the target vesicle. (d–f) Schematics illustrating the experiment shown in g–j. Membrane material is added to a vesicle container connected to two nanotubes, both of which are dilated when the tension drops. By increasing the membrane tension in a target vesicle, the nanotube-integrated vesicles move toward it, following the lipid flow. (g) Nomarski DIC microscopy image of a nanofluidic switch. The image shows the network immediately after the nanotube-integrated vesicles have formed. White arrows show the location of these vesicles, and inset shows a magnified image of one nanotube. Lipid flow and concomitant vesicle transport is induced by deforming (increase in  $\sigma$ ) the vesicle down to the right ( $+F$ ) with a carbon fiber. Black arrows show net flow directions during the increased tension. Also shown (lower left) is the micropipet used for creating the networks and for injection of donor vesicles. The microscopy images shown in g–j are digitally processed and edited for clarity of presentation. (h) The nanotube-integrated vesicles have merged with the target vesicle. (i,j) The corresponding sequence with shape deformation (increase in  $\sigma$ ) of another target vesicle in the same network showing vesicle transport in another direction. Scale bar in g–l, 10  $\mu\text{m}$ . Inset scale bar in g–h, 5  $\mu\text{m}$ ; in i–j, 3  $\mu\text{m}$ . (k) Fluorescent dextrane was loaded into nanotube-integrated vesicles and transported toward a vesicle having no fluorescent dextrane (shown by dotted line). Flow direction is shown by white arrows. (l) The nanotube-integrated vesicle injecting its contents into the target vesicle. The microscopy images shown in g–j are digitally processed and edited for clarity of presentation. Scale bar g–l, 10  $\mu\text{m}$ . Inset scale bar g–h, 5  $\mu\text{m}$ ; i–j, 3  $\mu\text{m}$ .

perturbation technique for modulation of membrane tension, transport can be achieved between any two containers in a large

network. Molecules or colloidal particles, possibly down to the limit of single entities, can be shuttled through the network to different destinations, and the number of different pathways from start- to end-point through a network can be very large. In a simple doubly branching network, the number of pathways increases as  $2^n$ , where  $n$  is the level of branching. For example, in a doubly branching network, the number of pathways for the second level of branching is 4, and for the seventh level there are 128 different pathways. Through addition of three-way nanotube-junctions, or by increasing the connectivity toward fully connected networks, the number of pathways can increase even further. Since the chemical identity of each individual container can be controlled and easily changed,<sup>7</sup> the order and number of chemical operations that can be performed sequentially on the molecules transported through the networks are just as many.

In summary, a novel nanofluidic switching device, characterized by an extremely small size and consisting of a single lipid bilayer membrane, has been constructed. The device is capable of handling and injecting atto- to femtoliter volumes into selected reaction containers, and the “pumping action” is controlled by manipulation of the energy state of the device material itself. The ultra-small scale of the transport channels (approaching the scale of large molecules) and the precise control of transport through the networks make these systems ideally suited for performing complex manipulations of the solution environment around single molecules. Thus, in essence, a nanoscale chemical laboratory with the capability of working with a few or even single molecules can be designed on the basis of these networks.

## References

- (1) Chiu, D. T.; et al. *Science* **1999**, *283*, 1892.
- (2) Brody, J. P.; Yager, P.; Goldstein, R. E.; Austin, R. H. *Biophys. J.* **1996**, *71*, 3430.
- (3) LeDuc, P.; Haber, C.; Bao, G.; Wirtz, D. *Nature* **1999**, *399*, 564.
- (4) Lu, H. P.; Xun, L.; Xie, X. S. *Science* **1998**, *282*, 1877.
- (5) Wei, Q.-H.; Bechinger, C.; Leiderer, P. *Science* **2000**, *287*, 625.
- (6) Sciaky, N.; et al. *J. Cell Biol.* **1997**, *139*, 1137.
- (7) Ishii, Y.; Yanagida, T. *Single Mol.* **2000**, *1*, 5.
- (8) Karlsson, A.; Karlsson, R.; Karlsson, M.; Cans, A.-S.; Stromberg, A.; Ryttsen, F.; Orwar, O. *Nature* **2001**, *409*, 150.
- (9) Karlsson, M.; Sott, K.; Cans, A.-S.; Karlsson, A.; Karlsson, R.; Orwar, O. *Langmuir* **2001**, *17*, 6754.
- (10) Karlsson, M.; Sott, K.; Davidson, M.; Cans, A.-S.; Linderholm, P.; Chiu, D.; Orwar, O. *Proc. Natl. Acad. Sci. U.S.A.* **2002**, *99*, 11573.
- (11) Karlsson, R.; et al. *Langmuir* **2002**, *18*, 4186.
- (12) Cans, A.-S.; Wittenberg, N.; Karlsson, R.; Sombers, L.; Karlsson, M.; Orwar, O.; Ewing, A. *Proc. Natl. Acad. Sci. U.S.A.* **2003**, *100*, 400.
- (13) Rawics, W.; Olbrich, K. C.; McIntosh, T.; Needham, D.; Evans, E. *Biophys. J.* **2000**, *79*, 328.
- (14) Karlsson, R.; Karlsson, A.; Orwar, O. Formation and transport of nanotube-integrated vesicles in a nanoscale bilayer network. *J. Phys. Chem. B*, in press.
- (15) Chizmadzhev, Y. A.; Kumenko, D. A.; Kuzmin, P. I.; Chernomordik, L. V.; Zimmerberg, J.; Cohen, F. S. *Biophys. J.* **1999**, *76*, 2951.

JA0348748